



OPEN

Immunological characterization of a long-lasting response in a patient with metastatic triple-negative breast cancer treated with PD-1 and LAG-3 blockade

Licia Rivoltini¹, Chiara Camisaschi^{1,3}, Giovanni Fucà², Biagio Paolini⁴, Barbara Vergani⁵, Valeria Beretta¹, Silvia Damian², Matteo Duca², Sara Cresta², Michele Magni², Biagio Eugenio Leone⁵, Chiara Castelli¹, Filippo de Braud^{2,6}, Francesca De Santis^{2,7} & Massimo Di Nicola^{2,7}✉

In patients with advanced triple-negative breast cancer (TNBC), translational research efforts are needed to improve the clinical efficacy of immunotherapy with checkpoint inhibitors. Here, we report on the immunological characterization of an exceptional, long-lasting, tumor complete response in a patient with metastatic TNBC treated with dual PD-1 and LAG-3 blockade within the phase I/II study CLAG525X2101C (NCT02460224). The pre-treatment tumor biopsy revealed the presence of a CD3⁺ and CD8⁺ cell infiltrate, with few PD1⁺ cells, rare CD4⁺ cells, and an absence of both NK cells and LAG3 expression. Conversely, tumor cells exhibited positive staining for the three primary LAG-3 ligands (HLA-DR, FGL-1, and galectin-3), while being negative for PD-L1. In peripheral blood, baseline expression of LAG-3 and PD-1 was observed in circulating immune cells. Following treatment initiation, there was a rapid increase in proliferating granzyme-B⁺ NK and T cells, including CD4⁺ T cells, alongside a reduction in myeloid-derived suppressor cells. The role of LAG-3 expression on circulating NK cells, as well as the expression of LAG-3 ligands on tumor cells and the early modulation of circulating cytotoxic CD4⁺ T cells warrant further investigation as exploitable predictive biomarkers for dual PD-1 and LAG-3 blockade.

Trial registration: NCT02460224. Registered 02/06/2015.

The clinical studies evaluating anti-PD-1/PD-L1 monotherapy in triple-negative breast cancer (TNBC) have demonstrated a relatively modest level of activity compared to other histologies such as melanoma and non-small cell lung cancer NSCLC¹. This limited efficacy of PD-1/PD-L1 inhibitors alone may be attributed to the involvement of additional immune checkpoints in the process of cancer immunoediting. Consequently, there is growing interest in investigating combination approaches that target different and complementary immune checkpoints². Among these novel targets, the Lymphocyte Activation Gene-3 (LAG-3) stands out as a particularly promising surface molecule expressed on activated T and NK cells, which exerts negative regulation on immune effector

¹Unit of Immunotherapy of Human Tumors, Fondazione IRCCS Istituto Nazionale dei Tumori, Milan, Italy. ²Immunotherapy and Innovative Therapeutics Unit, Medical Oncology and Hematology Department, Fondazione IRCCS Istituto Nazionale dei Tumori, Via Giacomo Venezian, 1, 20133 Milan, Italy. ³Biomarkers Unit, Department of Applied Research and Technical Development, Fondazione IRCCS Istituto Nazionale dei Tumori, Milan, Italy. ⁴Pathology A Unit, Department of Pathology, Fondazione IRCCS Istituto Nazionale dei Tumori, Milan, Italy. ⁵Department of Medicine and Surgery, University of Milano-Bicocca, Monza, Italy. ⁶Oncology and Hemato-Oncology Department, University of Milan, Milan, Italy. ⁷These authors contributed equally: Francesca De Santis and Massimo Di Nicola. ✉email: massimo.dinicola@istitutotumori.mi.it

signaling upon ligand engagement³. In this report, we present a remarkable and durable complete response to dual PD-1/LAG-3 blockade observed in a patient with metastatic TNBC who participated in the phase I/II study CLAG525X2101C (NCT02460224)⁴.

Results

Dynamics of response to dual PD-1/LAG-3 blockade

The patient in their 60s was affected by heavily-pretreated metastatic TNBC with significant skin involvement and lymph nodal metastases. Figure 1A illustrates the dynamics of the clinical and radiological response to the dual PD-1/LAG-3 blockade. After three cycles of the experimental treatment, the first radiological tumor reassessment at week + 9 revealed a near-complete response (CR) of the lymph nodal metastases (Fig. 1B). This response was accompanied by regression in most of the sites of skin involvement. Supplemental Figure S1 displays H&E-stained tissue sections of tumor biopsy specimens (A) and the pathological complete response observed at week + 9 (B). At week + 18, a complete clinical response was achieved in the cutaneous lesions (Fig. 1C), and a RECIST CR was attained at week + 20. As of the data cutoff date for this report, the patient remains on treatment and has remained disease-free during a follow-up period of over 50 months.

Immune and molecular tumor characterization

To investigate the basis of this exceptional response, we conducted a characterization of the tumor's molecular and immunological profile. The tumor punch biopsy obtained at baseline from the skin localization on cycle 1 day 1 (CID1, prior to treatment initiation) revealed a zonal distribution of tumor-infiltrating lymphocytes (TILs) (Supplemental Fig. S1A), with a CD3+ T cell infiltrate ranging from 5 to 30% (Fig. 1D and Supplemental Fig. S2). This range was similar to the median of 20% TILs reported in the literature for TNBC⁵. TIL characterization showed a moderate presence of CD8⁺ T cells with rare CD4⁺ T cells and no detectable infiltration of NK and NKT cellular elements, as demonstrated by the absence of CD56 immunostaining (Fig. 1D). In terms of immune checkpoints, PD-1 expression was scanty and detectable only within the CD8⁺ T cell subset (Figs. 1D and 2A) while LAG-3 was absent in T and any other infiltrating immune cells (Supplemental Fig. S2E). It is worth mentioning that no expression of PD-L1 could be observed (Fig. 2B), whereas three (HLA-DR, FGL-1, and galectin-3) of the multiple ligands for LAG-3³ were highly expressed in both cancer and stromal cells (Fig. 1E and Supplemental Fig. S3A–C). The antigenic analysis of tumor cells revealed a microsatellite stable genotype (MSS+), indicating the absence of DNA hyper-mutability underlying the potential immunogenicity of the tumor through the expression of neoantigens⁶. However, the cancer testis antigen NY-ESO-1, which is typically well-represented in TNBC⁷, showed high positivity at tumor level (Figs. 1E, 3).

A tissue biopsy obtained from the responding tumor lesion, nine weeks after treatment initiation, showed no residual cancer cells confirming the complete regression, along with the presence of abundant stroma and histiocytes as detected by histological analysis (Supplemental Fig. S1B); however, no immune infiltrate could be observed, likely due to the late time point of the sampling.

By profiling peripheral blood mononuclear cells (PBMC), we observed that PD-1 was expressed in a significant proportion of CD4⁺ T and Treg cells (23% and 17%, respectively), while poorly represented in CD8⁺ T cells (3%); no detection of this immune checkpoint could instead be noticed in either CD56^{dim} cytotoxic NK or CD56^{high} cytokine-producer NK cell subsets (Fig. 4A). In contrast, LAG-3 was abundantly present in a remarkable fraction of Tregs (26%), a subset of CD8⁺ T (4%) and both the CD56^{high} and CD56^{dim} NK cell sub-populations (8% and 19% respectively) (Fig. 4A).

The dynamic immune monitoring of PBMC revealed that after the first infusion of the combo-therapy (CID1) and throughout the treatment (up to the 7th cycle), the number of circulating T and NK cells did not significantly change, while circulating Tregs (defined as CD3⁺CD4⁺CD25⁺Foxp3⁺ cells) showed a progressive boost, which is consistent with the occurrence of full-fledged immune-stimulation⁸ (Fig. 4B). Concomitantly, treatment was associated with a strong and rapid decrease in monocytic myeloid-derived suppressor cells (M-MDSCs, CD14⁺HLA-DR^{neg} cells), despite no significant change in the overall CD14⁺ monocytic population, and by a reduction of granulocytic MDSCs (PMN-MDSCs, CD14⁺CD15⁺CD11b⁺ low-density cells), indicating a lowering of the systemic immunosuppression associated with altered myelopoiesis (Fig. 4B). This immune scenario was paralleled by a remarkable increase in the fraction of Ki67⁺ and granzyme-B double-positive cells in CD4⁺ (3.8% pre vs 12.7% post) and CD8⁺ (5% pre vs 9.4% post) T lymphocytes, as well as in both the CD56^{high} (16.2% pre vs 35% post) and CD56^{dim} (6.4% pre vs 20.8% post) NK cell subsets (Fig. 4C), which suggests the ability of PD-1 and LAG3 blockade to unleash proliferating and cytotoxic anti-tumor effectors. This hypothesis is also supported by the evidence that circulating CD8⁺ T cells recognizing the tumor antigen NY-ESO-1, highly expressed on the TNBC cells of this patient (Fig. 1E), exhibited a sustained expansion during treatment as indicated by the staining with HLA-A*0201/NY-ESO-1 peptide pentamers (Fig. 4D). Finally, both CD4⁺ and CD8⁺ T cells showed a significant skew toward an effector-memory (CD45RA-CCR7⁻) phenotype (Fig. 4E), suggesting a potential ability of the combined PD-1 and LAG-3 inhibition to triggering systemic immunological memory.

Discussion

In this report, we present the case of a patient with TNBC who experienced a complete tumor regression when treated with a combination of PD-1 and LAG-3 blocking antibodies. In particular this case belongs to a phase I/II, open label, multicenter study investigating the safety and efficacy of the humanized immunoglobulin 4 (IgG4) anti-LAG3 mAb ieramimab (LAG525) ± the humanized IgG4 anti-PD-1 mAb spartalizumab (PDR001) in patients with advanced solid malignancies⁹.

The analysis of a skin lesion biopsied at baseline revealed a scanty and heterogeneous T cell infiltrate poorly expressing the targeted immune checkpoints PD-1 and LAG3, the absence of PD-L1 expression in both cancer or

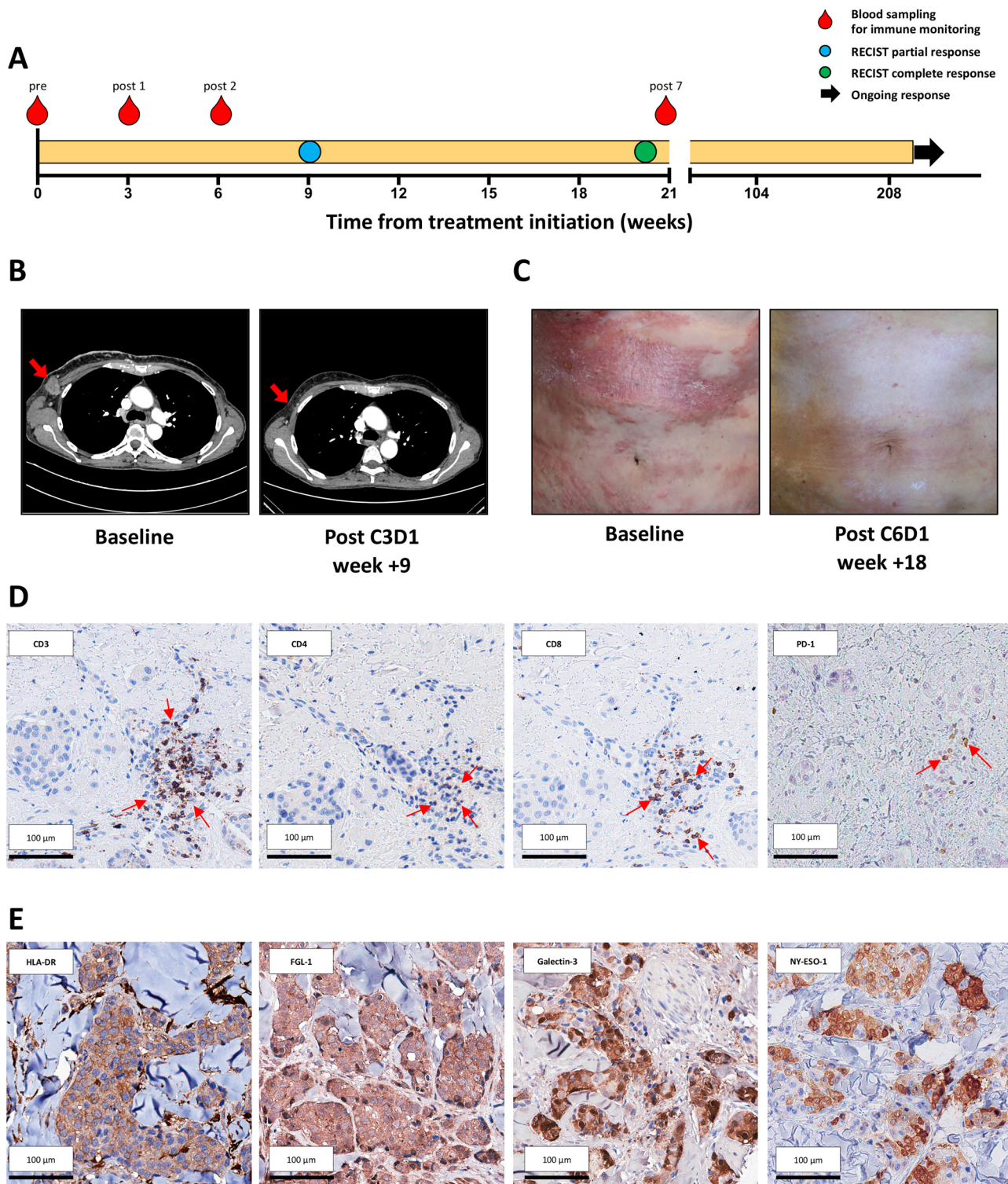


Figure 1. Dynamics of response to dual PD-1/LAG-3 blockade and immune-molecular tumor characterization. (A) Shows the timeline of response dynamics together with the time of blood sampling for the immune monitoring. A rapid antitumor activity with a radiological partial response (as illustrated by the computed tomography images of a lymph node metastases in B) was achieved at week +9 and was paralleled by the regression of most of the skin involvement. A complete clinical response of the extensive skin localization was observed at week +18 (C). A complete radiological response (as per RECIST v.1.1) was achieved at week +20. The immunohistochemical characterization of the tumor microenvironment showed a zonal CD3⁺ infiltrate mainly composed of CD8⁺ cells with rare CD4⁺ and rare PD-1⁺ cells (D, images at 20 × magnification). Tumor cells stained positive for the three main known LAG-3 ligands (HLA-DR, FGL-1 and galectin-3) and for the cancer testis antigen NY-ESO-1 (E, images at 20 × magnification).

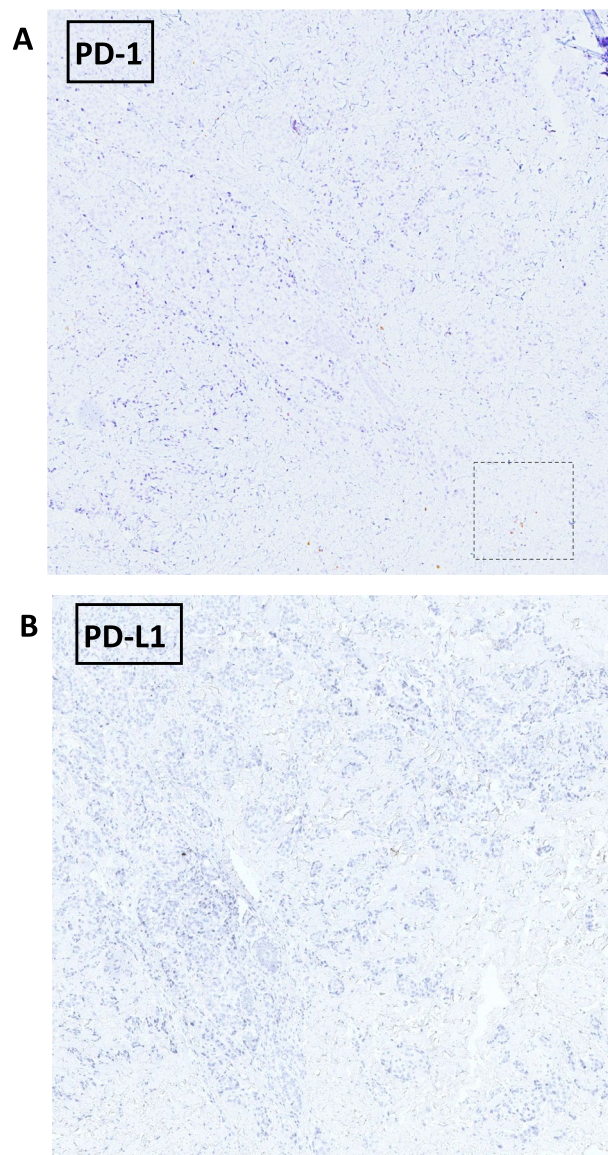


Figure 2. Immunohistochemical staining at 4× magnification. Immunohistochemical staining for PD-1 (A) and PD-L1 (B) at 4× magnification. The dashed line rectangle indicates the area showed at 20× magnification in Fig. 1D.

stromal cells, and a MSS genotype, which are all hallmarks of tumors poorly responding to PD-1/PD-L1 blockade monotherapy, as reported in multiple previous clinical trials¹. However, the high levels of three (HLA-DR, FGL-1, and galectin-3) of the putative LAG-3 ligands¹⁰ in cancer cells, confirming the involvement of these molecules in blunting antitumor immunosurveillance¹¹, points to the expression of HLA-DR, FGL-1, and/or galectin-3 as potential predictive factor of sensitivity to LAG3 blockade therapy.

As systemic immunity is acknowledged to impact of antitumor immune responses occurring at tumor site¹², baseline and dynamic immunoprofiling of peripheral blood was performed in the patient here depicted. A prevalent expression of LAG3 with respect to PD-1 was detected in pre-treatment PBMC, particularly in CD8+ T, Treg, and both CD56^{dim} and CD56^{high} NK cells. Based on this evidence, and the high levels of HLA-DR, FGL-1, and galectin-3 cognate ligands at tumor site, it is tempting to speculate that systemic LAG-3 blockade might have triggering an immunological cascade leading to the expansion of active immune effectors which would eventually migrate to tumor site to mediate the complete tumor regression observed in our patient, with PD-1 blocker possibly amplifying and prolonging the immunomodulating effect¹³. Indeed, the administration of LAG3 and PD-1 blocking mAbs was associated with a remarkable increase of multiple activated, cytotoxic and proliferating immune effectors including CD8⁺, CD4⁺ T and NK cells. If the activity of this immunotherapeutic strategy on T cells is expected based on the literature data¹⁰, we believe a novelty of this report might rely on the remarkable activation and expansion of both cytotoxic and cytokine-producing NK cells observed to occur rapidly upon treatment. These effectors, endowed with an antitumor potential in TNBC patients¹⁴, have been recently reported

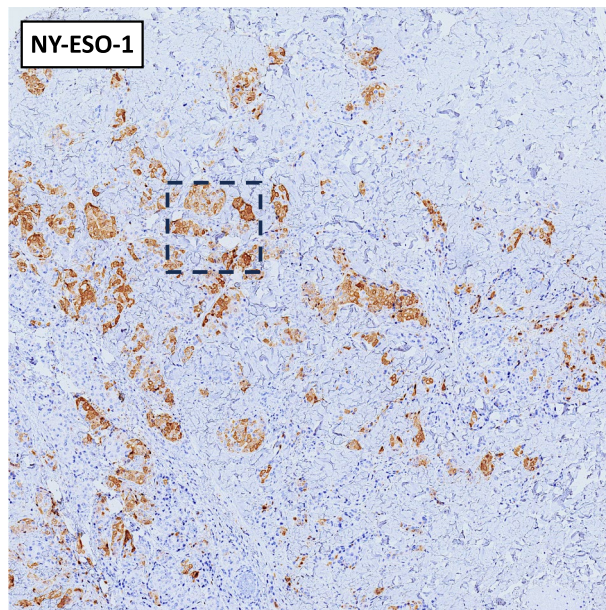


Figure 3. Immunohistochemical staining for NY-ESO-1 at 4× magnification. The dashed line rectangle indicates the area showed at 20× magnification in Fig. 1E.

to upregulate LAG3 and to acquire mature phenotype as well as effector functions upon LAG3 blockade¹⁵, thus representing a potential mediator of the antitumor activity triggered *in vivo* by LAG3 inhibition¹⁶.

The complete tumor regression experienced by this patient was also associated with a substantial modulation of regulatory and suppressive peripheral immune compartments. Notably, the boost of Treg, often paralleling full-fledged immune responses⁸, did not apparently impair the activation of T and NK effectors possibly due to the ability of LAG3 and PD-1 inhibition of making these cells resistant to immunosuppression *in vivo*¹⁷. In contrast, M-MDSC and PMN-MDSC rapidly dropped after the first treatment cycle, indicating a direct activity of LAG3/PD-1 blocking on the systemic myeloid population rather than an indirect effect due to the reduced tumor burden. Albeit the molecular mechanisms underlying this process require further investigation, it could be hypothesized that PD-1 expressed on myeloid cells may play a central role in orchestrating immune checkpoint blockade, as recently highlighted¹⁸; similarly, as Lag3 ligands are abundantly detectable on myeloid cells in different pathological conditions including breast cancer¹⁹ and soluble LAG3 is key in myeloid cell differentiation²⁰, blockade of this checkpoint might have also contributed to myeloid cell reprogramming from immunosuppressive to proinflammatory effectors endowed with antitumor potential^{21,22}.

In conclusion, based on the lesson learnt from a single case report, we speculate that the exceptional and long-lasting complete response achieved in this TNBC patient following dual PD-1/LAG-3 blockade may have been driven by a multifaceted immune response, including the reversal of NK cell exhaustion mediated by the LAG-3 axis, the reactivation of cytotoxic and effector-memory T lymphocytes, and the reprogramming or recirculation of myeloid cells. These findings suggest that PD-1/LAG-3 blockade could be an effective treatment approach for tumors expressing the hallmarks of PD-1 blockade resistance but high levels of LAG-3 ligands. Further investigations are needed to confirm whether the tumor and the blood pathways here identified at baseline or early during treatment may represent true predictive biomarkers for anti-LAG-3 blockade-based immunotherapy.

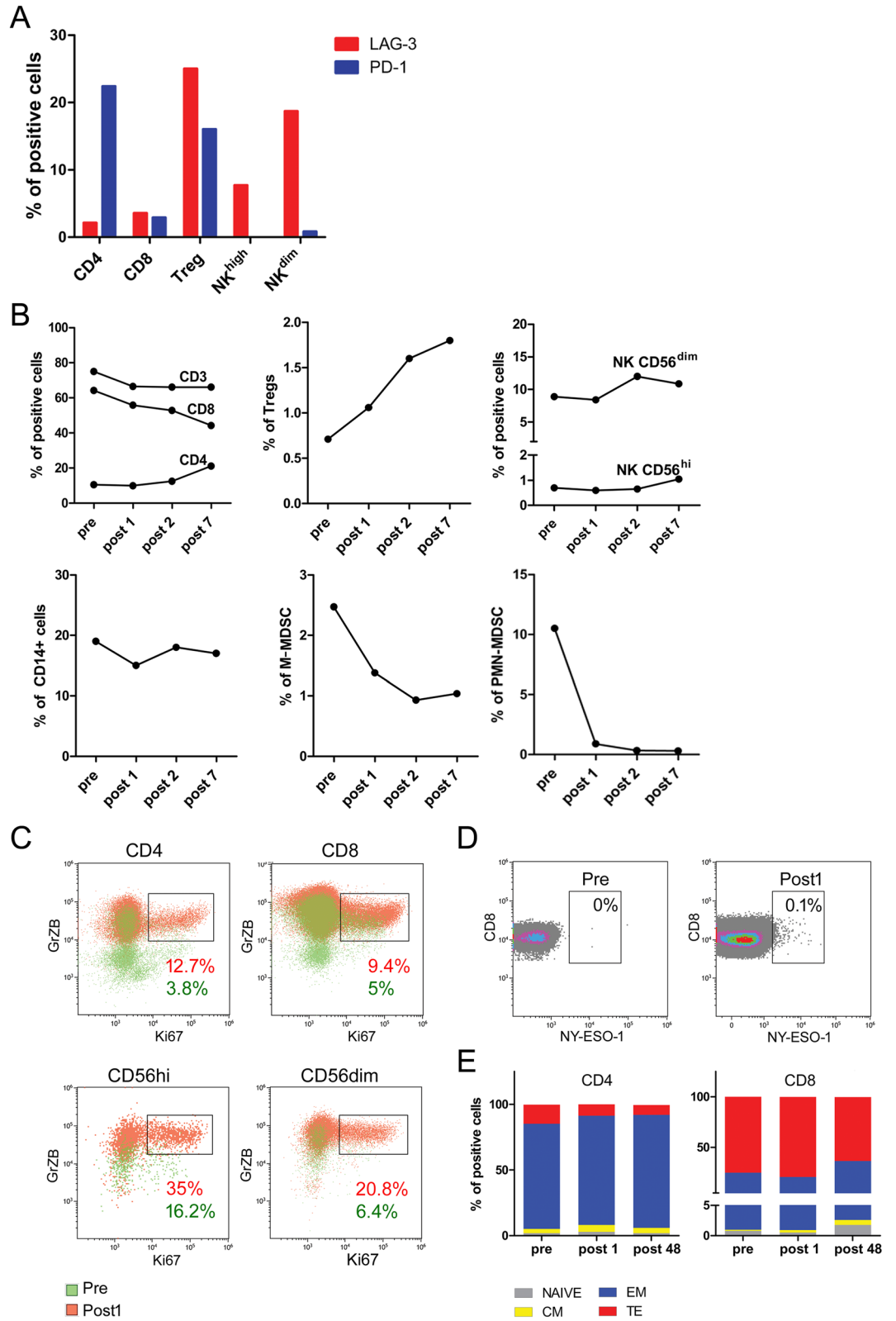
Methods

Experimental treatment

In June 2016, the patient started the experimental treatment regimen consisting of LAG525 (a humanized IgG4 anti-LAG-3 monoclonal antibody [mAb]) at a dosage of 240 mg, and spartalizumab (PDR001, a humanized IgG4 anti-PD-1 mAb) at a dosage of 300 mg, administered every three weeks. Tumor response was assessed using RECIST v1.1 criteria in accordance with the study protocol. The data cutoff date for the present report is 01/03/2023.

Formalin-fixed, paraffin-embedded (FFPE) tissue blocks were retrieved, and expert pathologist review was conducted on hematoxylin and eosin (H&E) stained tissue sections. Immunohistochemical characterization utilized the reagents listed in Supplemental Table S1. Antigen retrieval was performed at high temperatures (96–98 °C) using different buffers, and the antigen–antibody reaction was visualized using commercial detection kits (see Supplemental Table S1). Microsatellite instability (MSI) status was determined through polymerase chain reaction (PCR) following international guidelines⁵.

Peripheral blood mononuclear cells (PBMCs) were isolated from blood samples using Ficoll gradient (Leucosep polypropylene tubes, Thermo Fisher Scientific) within two hours from withdrawal. The reagents employed for cell staining are provided in Supplemental Table S2. Samples were analyzed using the Gallios Flow Cytometer,



◀ **Figure 4.** Effects of PD-1/LAG-3 dual blockade on blood immune cell frequency and induction of a lymphocyte-mediated antitumor response soon after treatment initiation. Freshly thawed PBMCs were analysed by flow cytometry. **(A)** Percentage of LAG-3 (red) and PD-1 (blue) positive cells at the baseline in CD4⁺, CD8⁺, Treg (CD4⁺CD25⁺Foxp3⁺) and NK cells (CD16⁻CD56^{hi} and CD16⁺CD56^{dim}) are reported in graph. **(B)** Frequency of lymphoid (CD3⁺, CD4⁺, CD8⁺, Treg, NK cells) and myeloid (CD14⁺ monocytes, M-MDSC and PMN-MDSC) populations at the baseline (pre) and after treatments (post 1, 2, 7) are shown. **(C)** overlay dot plots show the increased proliferation of GrZB⁺ cells (rectangle gate) after the first treatment (red) compared to the baseline (green) in CD4⁺ and CD8⁺ T cells (upper row) and in NK CD56^{hi} and NK CD56^{dim} (lower row). The frequency of cells expressing both the intracellular markers, Ki67 and GrZB, are reported in the graph as percentages (red = first treatment, green = baseline). **(D)** The presence of NY-ESO-1 specific CD8⁺ T cells was evaluated comparing PBMCs at the baseline and after the first treatment using HLA-A*0201/NY-ESO-1 multimer staining. The percentage of CD8⁺ multimer positive cells was calculated in the CD8⁺CD19⁻ gate and reported in the figure. **(E)** PBMCs were stained with a combination of mAbs to define naïve and memory T cell subsets. Histograms show the percentage of naïve (CD45RA⁺CCR7⁺, grey), effector memory (EM, CD45RA⁻CCR7⁻, blue), central memory (CM, CD45RA⁻CCR7⁺, yellow) and terminally effector (TE, CD45RA⁺CCR7⁻, red) cells in CD4⁺ and CD8⁺ lymphocytes at the baseline (pre), after the first treatment (post 1) and late in the treatment (post 48).

and the Kaluza software (Beckman Coulter) was used for data analysis. Positive cells were identified within the live cell population after doublet discrimination, and based on fluorescence minus one (FMO) control.

Data availability

The data generated and/or analyzed during the current study are available from the corresponding author on reasonable request.

Received: 6 November 2023; Accepted: 7 February 2024

Published online: 09 February 2024

References

- Keenan, T. E. & Tolaney, S. M. Role of immunotherapy in triple-negative breast cancer. *J. Natl. Compr. Cancer Netw.* **18**(4), 479–489 (2020).
- Fucà, G., de Braud, F. & Di Nicola, M. Immunotherapy-based combinations: an update. *Curr. Opin. Oncol.* **30**(5), 345–351 (2018).
- Maruhashi, T., Sugiura, D., Okazaki, I. M. & Okazaki, T. LAG-3: from molecular functions to clinical applications. *J. Immunother. Cancer* **8**(2), e01001014 (2020).
- Hong, D. S. *et al.* Phase I/II study of LAG525 ± spartalizumab (PDR001) in patients (pts) with advanced malignancies. *J. Clin. Oncol.* **36**(15_Suppl), 3012 (2018).
- Pruneri, G. *et al.* Clinical validity of tumor-infiltrating lymphocytes analysis in patients with triple-negative breast cancer. *Ann. Oncol.* **27**(2), 249–256 (2016).
- Luchini, C. *et al.* ESMO recommendations on microsatellite instability testing for immunotherapy in cancer, and its relationship with PD-1/PD-L1 expression and tumour mutational burden: a systematic review-based approach. *Ann. Oncol.* **30**(8), 1232–1243 (2019).
- Ademuyiwa, F. O. *et al.* NY-ESO-1 cancer testis antigen demonstrates high immunogenicity in triple negative breast cancer. *PLoS ONE* **7**(6), e38783 (2012).
- Koh, J. *et al.* Regulatory (FoxP3⁺) T cells and TGF-β predict the response to anti-PD-1 immunotherapy in patients with non-small cell lung cancer. *Sci. Rep.* **10**(1), 18994 (2020).
- Schöffski, P. *et al.* Phase I/II study of the LAG-3 inhibitor ieramilimab (LAG525) ± anti-PD-1 spartalizumab (PDR001) in patients with advanced malignancies. *J. Immunother. Cancer* **10**, e003776 (2022).
- Graydon, C. G., Moideen, S. & Fowke, K. R. LAG3's enigmatic mechanism of action. *Front. Immunol.* **11**, 5317 (2021).
- Girotti, M. R., Salatino, M., Dalotto-Moreno, T. & Rabinovich, G. A. Sweetening the hallmarks of cancer: Galectins as multifunctional mediators of tumor progression. *J. Exp. Med.* **217**(2), e20182041 (2020).
- Hiam-Galvez, K. J., Allen, B. M. & Spitzer, M. H. Systemic immunity in cancer. *Nat. Rev. Cancer* **21**, 345–359 (2021).
- Ribas, A. *et al.* PD-1 blockade expands intratumoral memory T cells. *Cancer Immunol. Res.* **4**(3), 194–203 (2016).
- Abdel-Latif, M. & Youness, R. A. Why natural killer cells in triple negative breast cancer?. *World J. Clin. Oncol.* **11**(7), 464–476 (2020).
- Narayanan, S. *et al.* LAG3 is a central regulator of NK. Cell cytokine production. *bioRxiv* 2020.01.31.928200 (2020).
- Baixeras, E. *et al.* Characterization of the lymphocyte activation gene 3-encoded protein. A new ligand for human leukocyte antigen class II antigens. *J. Exp. Med.* **176**(2), 327–37 (1992).
- Durham, N. M. *et al.* Lymphocyte activation gene 3 (LAG-3) modulates the ability of CD4 T-cells to be suppressed in vivo. *PLoS ONE* **9**(11), e109080 (2014).
- Rudd, C. A new perspective in cancer immunotherapy: PD-1 on myeloid cells takes center stage in orchestrating immune checkpoint blockade. *Sci. Immunol.* **5**(43), eaaz8128 (2020).
- Liu, D. *et al.* LSECtin on tumor-associated macrophages enhances breast cancer stemness via interaction with its receptor BTN3A3. *Cell Res.* **29**, 365–378 (2019).
- Buisson, S. & Triebel, F. LAG-3 (CD223) reduces macrophage and dendritic cell differentiation from monocyte precursors. *Immunology* **114**(3), 369–374 (2005).
- Nieminen, J., St-Pierre, C. & Sato, S. Galectin-3 interacts with naïve and primed neutrophils, inducing innate immune responses. *J. Leukoc. Biol.* **78**(5), 1127–1135 (2005).
- Gittens, B. R., Bodkin, J. V., Nourshargh, S., Perretti, M. & Cooper, D. Galectin-3: A positive regulator of leukocyte recruitment in the inflamed microcirculation. *J. Immunol.* **198**(11), 4458–4469 (2017).

Author contributions

G.F., C.Cam., Fd.B., C.Cas. and M.D.N. performed the conception and design of the study. C.Cam., B.P., B.V., V.B., S.D., M.D., S.C., M.M., B.E.L. and F.D.S. collected the data. G.F., C.Cam., B.P., B.V., B.E.L., L.R., C.C., F.D.S.

and M.D.N. analyzed and interpreted the data. G.F., C.Cam. wrote the draft of the manuscript. All authors reviewed the manuscript.

Competing interests

The authors declare no competing interests.

Additional information

Supplementary Information The online version contains supplementary material available at <https://doi.org/10.1038/s41598-024-54041-9>.

Correspondence and requests for materials should be addressed to M.N.

Reprints and permissions information is available at www.nature.com/reprints.

Publisher's note Springer Nature remains neutral with regard to jurisdictional claims in published maps and institutional affiliations.



Open Access This article is licensed under a Creative Commons Attribution 4.0 International License, which permits use, sharing, adaptation, distribution and reproduction in any medium or format, as long as you give appropriate credit to the original author(s) and the source, provide a link to the Creative Commons licence, and indicate if changes were made. The images or other third party material in this article are included in the article's Creative Commons licence, unless indicated otherwise in a credit line to the material. If material is not included in the article's Creative Commons licence and your intended use is not permitted by statutory regulation or exceeds the permitted use, you will need to obtain permission directly from the copyright holder. To view a copy of this licence, visit <http://creativecommons.org/licenses/by/4.0/>.

© The Author(s) 2024